EFFECTIVE RANGE APPROXIMATION IN VARIABLE PHASE APPROACH FOR TRIPLET ${}^3S_1^{\{np\}}$ AND SINGLET ${}^1S_0^{\{nn,np,pp\}}$ STATE

ANIL KHACHI

Chandigarh Group of Colleges Jhanjeri, Mohali, Punjab, India- 140307
Chandigarh Engineering College, Department of Applied Science
Corresponding author: anilkhachi1990@gmail.com

Received March 28, 2025

Abstract. This paper presents the application of the variable phase approach (VPA) to calculate phase shifts for various states: ${}^3S_1 - np$, ${}^1S_0 - nn$, ${}^1S_0 - np$, and ${}^1S_0 - pp$ using the effective range approximation potential. No free fitting parameters are used in the calculations, and a reasonably good match with the experimental phase shifts is observed for $E \leq 20\,\text{MeV}$, making the effective range approximation potential a strong candidate for obtaining low-energy scattering phase shifts. VPA employed is a powerful technique that *bypasses* the well known Schrödinger equation and does not require the wave function for SPS calculations, unlike the R-Matrix, S-Matrix, or Jost method. Interaction potentials are obtained for n-n, n-p, and p-p scattering that are exponential well-shaped.

Key words: Variable phase approach, Effective range approximation, NN interactions, amplitude functions, wave functions.

DOI: https://doi.org/10.59277/RomJPhys.2025.70.305

1. INTRODUCTION

The nucleon-nucleon interaction is one of the most fundamental problems in nuclear physics, yet it is not fully understood. Nuclear physicists demands precision potentials that has a capability to obtain the properties of the interacting systems as well has predictive power. After Yukawa [1] oldest theory of nucleon nucleon (NN) interactions which was based on mesons exchange, certain high class potentials were introduced like: Av-18, Nijm-I,II and III, CD-Bonn, Paris-Group, Hamada-Johnston, Yale-Group, Urbana-Group and Sao Paulo-Group CHPT potentials are having the capability to fit experimental data for other lighter systems [2]. Recently Granada group [3] has performed partial wave analysis on 6713 published np and pp scattering data below 350 MeV (from 1950-2013), thus helped to construct the inverse potentials more accurately. Aoki *et al.* have extracted the NN, hyperon potentials and the meson-baryon potentials potentials using lattice QCD [4, 5].

The experimental setup in neutron-neutron scattering consists of a neutron beam generated by ${}^3\text{H}(d,n)^4\text{He}$ reaction [6]. The target consists of heavy water enriched in D_2O. In total the $nd-$breakup reaction *i.e.*, $n + d(deuterium) \rightarrow p + n + n$ is the reaction leading to the appearance of interacting two neutrons in the final state. For

Table 1

Table represents various NN interactions taken up in this paper and different reactions responsible for producing desired projectiles. Last column presents the targets used in the scattering processes

Reaction	Projectile Production by	Projectile	Target
n-n [6]	^{3}H(d,n)^{4}He	n	D_2O
n-p [7]	^{2}H(p,n)2p	n	H in CH_2
p-p [8]	Ionizing hydrogen gas	p	H in CH_2, W , -$(C_2H_4)_n$- or graphite

various NN intercations Table 1 presents projectile production reactions and targets used.

Understanding neutron-neutron interaction is important because the reaction helps in the investigation of charge independence which has been fundamentally interesting to the nuclear community. It is well known that to investigate the charge independence in nuclear forces it is quite sufficient to compare the *np* and *pp* interactions. It is also known that to get more accurate information about these forces one needs to get precise low energy scattering data. Under such circumstances only S-waves are particularly important. The investigation of low energy scattering parameters is directly related to test the hypothesis of charge independence and charge symmetry. Both theoreticians and experimentalists are keen to precisely determine the low energy parameters for *np, pp* and *nn* interactions.

The nucleon-nucleon interactions at low energies are usually expressed in terms of effective range (r_e) and scattering length (a). These parameters provides information on the charge independence of the nuclear forces. There have been various arguments regarding the possibility of violation of charge independence and charge symmetry and some of them are discussed here:

- Darewych *et al.* [9] found that there was substantial difference between the *np* and *nn* potential curves with $^1S_0 - nn$ ($V_0 = 40.38$ MeV) and for $^1S_0 - np$ ($V_0 = 61.99$ MeV) hence observed "violation of charge independence". The violation was credited to the unavailability of high energy *nn* data. They used high energy *np* and *pp* data for fitting the *nn* SPS curve.
- Henley and others [10] have discussed about the small departure from charge symmetry and charge independence. The departure can be originated by *em* forces and is related to the basic understanding nuclear interaction and is ultimately connected with the fundamental particle principles of elementary physics. Since departures has been observed to be very small it was imperative to acquire precise data on the nucleon nucleon interaction.
- Babenko and Petrov [11] observed from a comparison of the low-energy parameters for the *np* system and their counterparts *pp* and *nn* systems that the charge dependence of nuclear forces is violated, which is associated with the mass difference

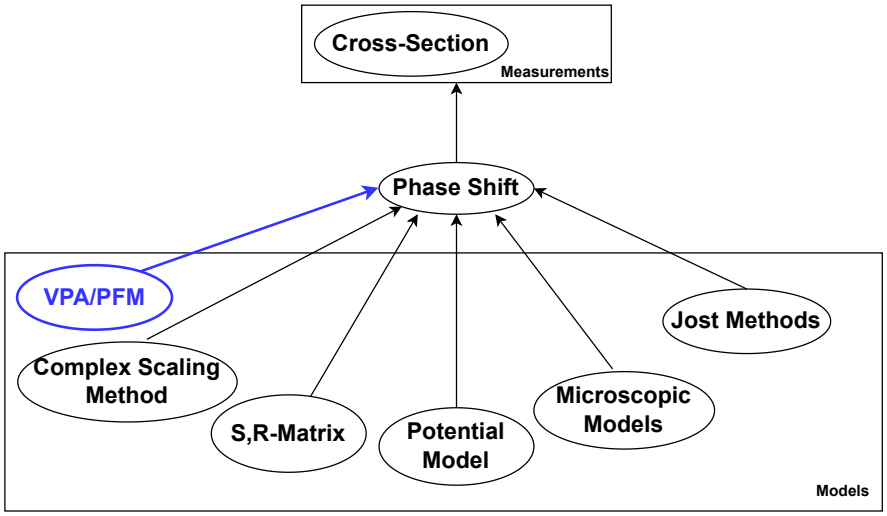

Fig. 1 – Different models found in the literature to obtain cross-section. In this work, we have employed a variable phase approach (VPA) that is wave function independent while the rest like R-matrix, S-matrix, complex scaling method, Jost method, potential model are wave function dependent.

between the charged and neutral pions.

- The values of scattering length and effective range are sensitive to any small change in n-n potentials. As stated by E.S. Konobeevski *et al.* [12]: "*A change of 7% in V(r) may lead to change of 20-30% in the scattering length calculation*".

The above mentioned points are either related to the precise knowledge of scattering data or related to the fundamental knowledge of elementary physics. Experimentally it has been observed that the p-p scattering [8] is even qualitatively very different from the n-p scattering. Because the Pauli principle excludes triplet states of even orbital angular momentum and singlet states of odd angular momentum. From the p-p scattering it is not possible to conclude directly that the n-p and p-p interactions are different. However there are arguments which make it seem fairly plausible that these interactions are indeed different. Our main aim in this paper is to use Calogero's variable phase approach (VPA) and to look for energy range where effective range approximation (ERA) potential is able to fit the experimental SPS data. Typically various methods are used to obtain the scattering phases by solving the Schrödinger equation, like the R-Matrix method, Jost method, Complex scaling method, Born approximation, Brysk's approximation, and other successive approximation techniques. These methods for phase shift and hence cross-section calculations have been shown in Fig. 1 which are wave function dependent.

The variable phase method (VPA), a technique for calculating scattering phase

shifts in nonrelativistic quantum mechanical scattering theory, has been in use for over 90 years and serves as a significant alternative to the direct integration of the radial Schrödinger equation. However, as emphasized by Calogero, this method remains underappreciated. Palov *et al.* have described it as "*the only exact method for the **direct** calculation of the scattering phase shift*" [13]. With the advancement of artificial intelligence the interaction potentials are also estimated using convolution neural networks [14–16].

In our earlier work we have applied variable phase approach (only potential dependent) for various scattering systems like $n-n$, $n-p$, $n-\alpha$, $n-d$, $\alpha-\alpha$, $\alpha-^3He$ and astrophysically important reaction $\alpha-^3He$ scattering systems [18–28] where Variational Monte-Carlo methods and genetic algorithms have been employed for the optimization process [29–31]. We have also obtained $n-p$ quantum mechanical functions like amplitude and wave function for various n-p channels and are in good agreement to that of Av-18 potential [32]. The present work shows how VPA is different from other well known wave function dependent methods (presented in Fig. 1) and how *'effective range approximation interaction potential'* works for low energy phase shift without need to optimize any potential parameter.

2. METHODOLOGY

We know from well known formula for effective range approximation [11]:

$$k\cot(\delta) = -\frac{1}{a} + \frac{1}{2}kr_e^2, \tag{1}$$

where a and r_e are scattering length and effective range whose numerical values are taken from [11]. If use is made of the approximation specified by Eq. 1, the S matrix can be written in the form [11]:

$$S(k) = \left(\frac{k+i\alpha}{k-i\alpha}\right)\left(\frac{k+i\beta}{k-i\beta}\right) \tag{2}$$

Where S(k) is related to scattering length a and effective range r_e by following relations

$$\alpha = \frac{1}{r_e}\left[1-\left(1-\frac{2r_e}{a}\right)^{1/2}\right] \tag{3}$$

$$\beta = \frac{1}{r_e}\left[1+\left(1-\frac{2r_e}{a}\right)^{1/2}\right] \tag{4}$$

The velocity independent or static potential corresponding to effective range approximation (ERA) given by [11]

$$V_{NN}(r) = -V_{NN0}\frac{e^{-r/R_{NN}}}{(1+\gamma e^{-r/R_{NN}})^2} \tag{5}$$

where

$$R_{NN} = \frac{1}{2\beta} \tag{6}$$

$$V_{NN0} = \frac{\hbar^2}{m_{NN}} \frac{\gamma}{R_{NN}^2} \tag{7}$$

$$\gamma = \frac{1+2\alpha R_{NN}}{1-2\alpha R_{NN}} \tag{8}$$

In above equations m_{NN} is the reduced mass of nucleonic system nn, np and pp. The effective potential in Eq. (5) will be introduced inside VPA equation as discussed below.

2.1. VARIABLE PHASE APPROACH (VPA)

The Schrödinger wave equation for a spinless particle with energy E and orbital angular momentum ℓ undergoing scattering is given by

$$\frac{\hbar^2}{2\mu}\left[\frac{d^2}{dr^2} + \left(k^2 - \ell(\ell+1)/r^2\right)\right] u_\ell(k,r) = V(r) u_\ell(k,r) \tag{9}$$

Where $k_{c.m} = \sqrt{E_{c.m}/(\hbar^2/2\mu)}$, $\hbar^2/2\mu$ = 41.47 MeV fm^2, ℓ indicates the orbital quantum number, $V(r)$ is the pair interaction potential (as given in Eq. (5)) and the energy of projectile E_{lab} is converted into center of mass energy $E_{c.m.}$ for non-relativistic kinematics as $E_{c.m} = \frac{M_p}{M_n+M_p} E_{lab}$. Second order differential equation Eq. (9) has been transformed to the first order non-homogeneous differential equation of Riccati type [33, 34] given by following equation:

$$\delta'_\ell(k,r) = -\frac{V(r)}{k\,(\hbar^2/2\mu)}\left[\cos(\delta_\ell(k,r))\hat{j}_\ell(kr) - \sin(\delta_\ell(k,r))\hat{\eta}_\ell(kr)\right]^2 \tag{10}$$

Here Prime denotes differentiation of phase function with respect to distance. Equation (10) will be used as our main tool for studying the properties of scattering phase shifts for n-p and p-p system. The advantage of the variable phase approach is that using the well known traditional approaches, one integrates the radial Schrödinger equation from the origin to the asymptotic region where the potential $V(r)$ is negligible, and then compares the phase of the radial wave function with that of a free wave and thus obtain the phase shift. In the variable phase approach we need only integrate a first-order nonlinear differential equation from the origin to the asymptotic region, thereby obtaining directly the value of the scattering phase shift. In integral form, the VPA equation or "phase equation" can be written as

$$\delta(k,r) = -\frac{1}{k\,(\hbar^2/2\mu)} \int_0^r V(r)\left[\cos(\delta_\ell(k,r))\hat{j}_\ell(kr) - \sin(\delta_\ell(k,r))\hat{\eta}_\ell(kr)\right]^2 dr. \tag{11}$$

Equation (10) is numerically solved using Runge-Kutta 5^{th} order (RK-5) method subjected to condition $\delta_\ell(0) = 0$. The above equation can be used to evaluate the phase function $\delta(r)$, which defines the total phase shift up to r. Then the phase shift (solution of a non-linear differential equation) is the limiting value

$$\delta = \lim_{r\to\infty} \delta_\ell(r). \tag{12}$$

To calculate δ the phase function $\delta(k,r)$ is evaluated up to a cut-off point at which $\delta(k,r)$ saturates or stabilizes. The function $\delta_\ell(r)$ does have a limit as $r \to \infty$ and that limit is the desired extracted phase shift. The physical implication of the cut-off point is that it is the radial distance beyond which the inter-nuclear potential can be considered zero. For $\ell = 0$, the Riccati-Bessel and Riccati-Neumann functions $\hat{j}_0$ and $\hat{\eta}_0$ get simplified as $\sin(kr)$ and $-\cos(kr)$, so Eq. (10), for $\ell = 0$ becomes

$$\delta_0'(k,r) = -\frac{V(r)}{k\,(\hbar^2/2\mu)} \sin^2[kr + \delta_0(k,r)] \tag{13}$$

In the above equation, the function $\delta_0(k,r)$ was termed "Phase function" by Morse and Allis [35]. Because the nucleon-nucleon interactions are short range, we integrate our phase shift equations to a distance of about 5 fm where the nucleon-nucleon potential becomes very weak. The equation for amplitude function [17, 18] with the initial condition $A_\ell(0) = 1$ is obtained in the form

$$\begin{aligned} A_\ell'(r) = &-\frac{A_\ell V(r)}{k}\left[\cos(\delta_\ell(k,r))\hat{j}_\ell(kr) - \sin(\delta_\ell(k,r))\hat{\eta}_\ell(kr)\right] \\ &\times\left[\sin(\delta_\ell(k,r))(\hat{j}_\ell(kr) + \cos(\delta_\ell(k,r))\hat{\eta}_\ell(kr)\right] \end{aligned} \tag{14}$$

for $\ell = 0$ amplitude function becomes

$$\begin{aligned} A_0'(r) = &-\frac{A_0 V(r)}{k\left(\frac{\hbar^2}{2\mu}\right)}\left[\cos\delta_0 \cdot \sin(kr) - \sin\delta_0 \cdot (-\cos(kr))\right] \\ &\times\left[\sin\delta_0 \cdot \sin(kr) + \cos\delta_0 \cdot (-\cos(kr))\right] \end{aligned} \tag{15}$$

also, the equation to obtain wave function is

$$u_\ell(r) = A_\ell(r)\left[\cos(\delta_\ell(k,r))\hat{j}_\ell(kr) - \sin(\delta_\ell(k,r))\hat{\eta}_\ell(kr)\right] \tag{16}$$

For $\ell = 0$ the wave function takes the following form

$$u_0(r) = A_0(r)\left[\cos\delta_0(r) \cdot \sin(kr) - \sin\delta_0(r) \cdot \cos(kr)\right] \tag{17}$$

Detailed flowchart to obtain phase shift, amplitude and wave function has been shown in Fig. 2.

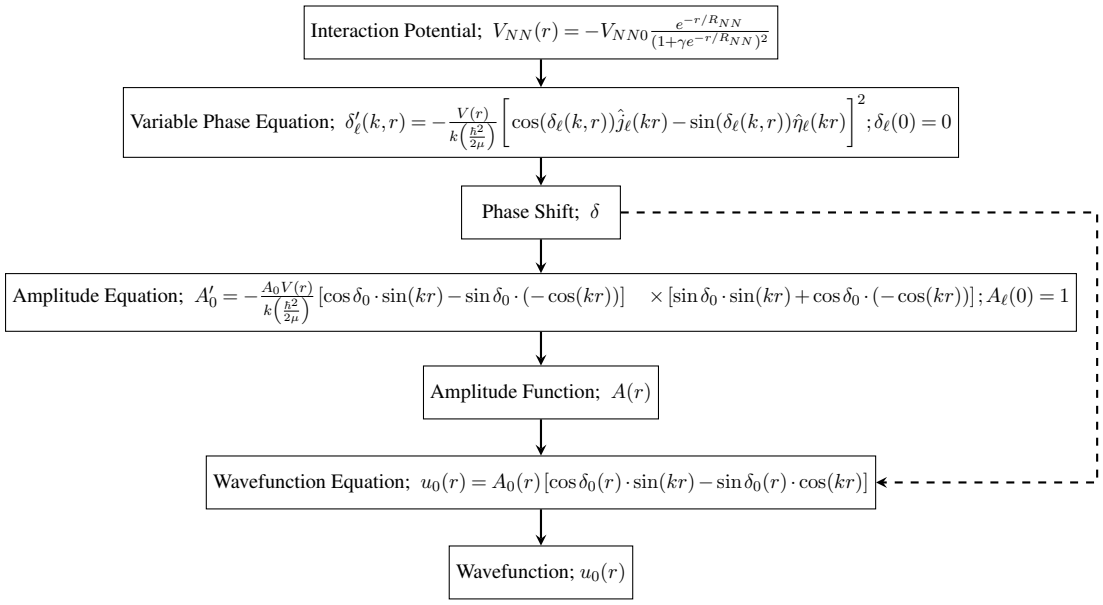

Fig. 2 – Detailed flowchart for obtaining phase shift, amplitude function, and wavefunction for n-p and p-p scattering.

2.2. PSEUDO-CODE FOR VARIABLE PHASE APPROACH

This stage involves writing an algorithm or pseudo-code as its first step. Let us identify the broad blocks of the algorithm as:

1. Initialization
2. Potential Definition
3. Function Definition
4. RK-5 procedure
5. Outputs

Algorithm as Pseudo code:

1. **Initialization**
   Set values for object variables:

```
mn = 939.565379 MeV/c^2
mp = 938.272046 MeV/c^2

Elab = [1, ..., 300, 350]
ObjVar = [mn, mp, Elab]
```

   Set values for interaction variables (Here ${}^1S_0 - np$ from [11]):

```
a= -23.71 fm
re = 2.70 fm
Vparam = [a, re]
```

Set values for state variables (Here ${}^1S_0 - np$ from reference [3] table 5):

```
deltaExpt = [62.105, ..., 1.982, -3.855, -8.923]
```

2. Potential Definition

```
def potential(r, Vparam):
    a = Vparam[0]
    re = Vparam[1]
    return V_{NN}....{use Eq. 5 as shown in page 4}
```

3. Function Definition

```
def f(r, delta0, Vparam, ObjVar):
    mn, mp, Elab = ObjVar
    muD = (mn * mp) / (mn + mp)
    hbarc = 197.329
    fac = (hbarc ** 2) / (2 * muD)
    ECoM = np.array(Elab) * mn / (mn + mp)
    k = np.sqrt(ECoM / fac)
    V = potential(r, Vparam)
    return (-V * np.sin(k * r + delta0) ** 2) / (k * fac)
```

4. VPA using RK-5

```
def VPARK5(Vparam, deltaExpt, ObjVar):
 h = 0.01
 r0 = 0.01
 rf = 5
 delta0 = 0

for r in np.arange(r0, rf, h):
 F1 = f(r, delta0, Vparam, ObjVar)
 F2 = f(r + h / 4, delta0 + h * F1 / 4, Vparam, ObjVar)
 F3 = f(r + h / 4, delta0 + h * (F1 / 8 + F2 / 8), Vparam, ObjVar)
 F4 = f(r + h / 2, delta0 - h * F2 / 2 + h * F3, Vparam, ObjVar)
 F5 = ....
 F6 = ....

 delta1 = delta0 +
            h * (7 * F1 + 32 * F3 + 12 * F4 + 32 * F5 + 7 * F6) / 90
 delta0 = delta1

 deltaObt = delta0 * 180 / np.pi
 return deltaObt
```

5. Outputs

```
import matplotlib.pyplot as plt

deltaObt = VPARK5(Vparam, deltaExpt, ObjVar)
plt.plot(Elab, deltaExpt, '*', label='Experimental')
plt.plot(Elab, deltaObt, label='Obtained')
plt.legend()
plt.show()
```

Make a call to the function: `deltaObt = VPARK5(Vparam, deltaExpt, ObjVar)` to obtain SPS corresponding to various lab energies `Elab`. After obtaining SPS one can easily obtain amplitude function and wave function by using Eqs. (15) and (17).

3. RESULTS AND DISCUSSION

For $^3S_1$ state we can see from Fig. 3 that the SPS are in excellent match with analysis data of both Wiringa *et al.* [36] and Granada group [3] upto 20 MeV of projectile energy in laboratory frame. The corresponding potential for $^3S_1$ state is shown in Fig. 7, where depth of around 70 MeV is observed. For $^1S_0$-nn and np again the SPS are in good match with Wiringa *et al.* and Granada as shown in Figs. 4 and 5. After 20 MeV the deviations can be clearly seen in Figs. 4 and 5 indicating the absence of repulsive core which becomes important at higher energies. Finally for $^1S_0$-pp state the SPS are in reasonably accuracy with Wiringa *et al.* and Granada group. The combined potentials for all $^1S_0$-nn, np and pp state can be seen in Fig. 7 to be very tightly packed with each other indicating the charge independence hypothesis of nuclear force.

It is observed that all the SPS are positive and their corresponding potentials are negative indicating that positive phase shifts will have attractive interactions which is in accordance to the main VPA equation. This point is of great pedagogic value as we can just by observing the nature $(+/-)$ of SPS can predict the nature of the interaction potential $(-/+)$ [37]. But above statement is not stringent as the results may change for potential having both attractive part and repulsive core as well as for higher values of wavenumber k.

After obtaining the scattering phase shifts we have employed Eqs. (13), (15) and (17) to obtain $\delta(r)$, amplitude function $A(r)$ and wavefunction u_0 for only $^1S_0 - np$ state as shown in Fig. 8.

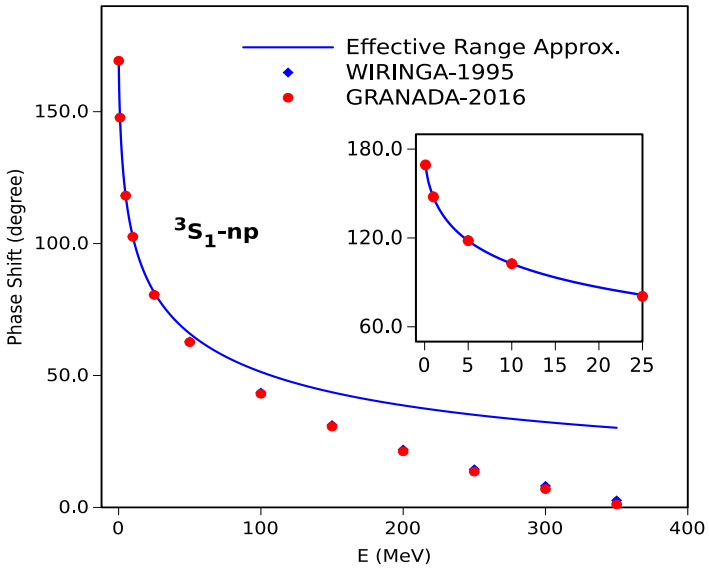

Fig. 3 – Bound triplet state ${}^3S_1 - np$ phase shift variation in comparison to experimental data from WIRINGA-1995 [36] and GRANADA-2016 [3].

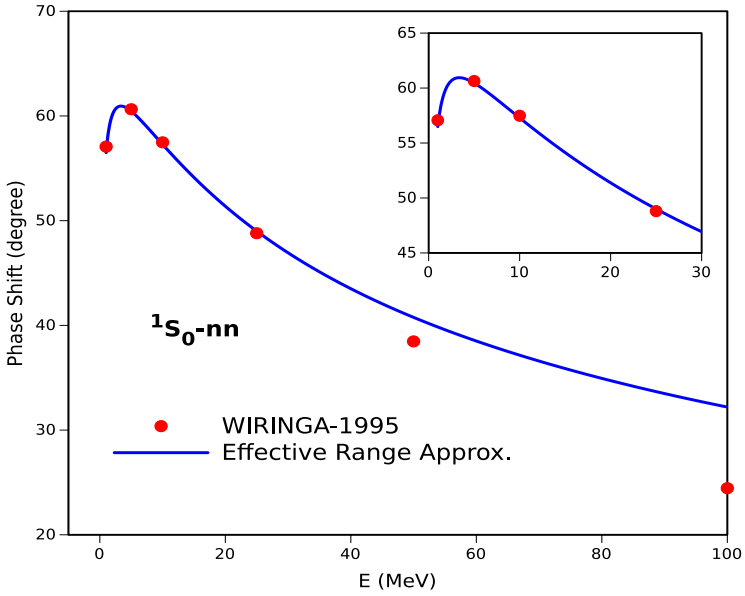

Fig. 4 – Singlet state ${}^1S_0 - nn$ phase shift variation in comparison to experimental data from WIRINGA-1995 [36].

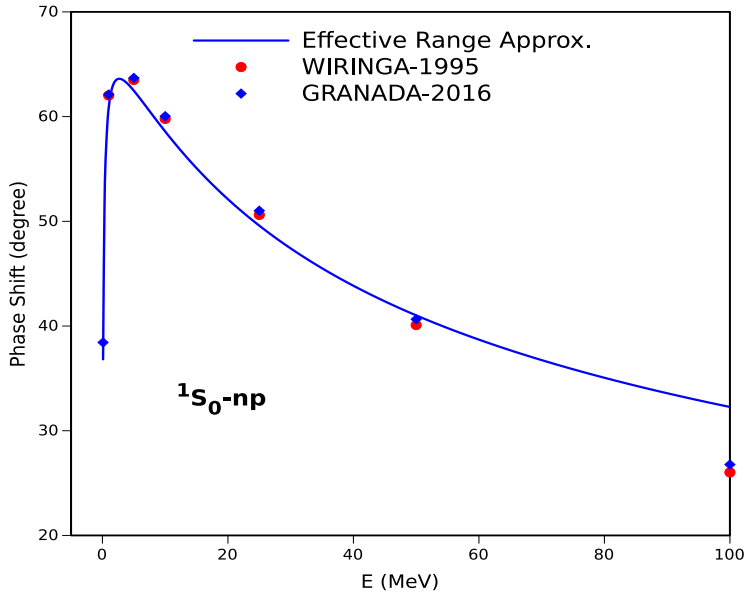

Fig. 5 – Singlet state ${}^1S_0 - np$ phase shift variation in comparison to experimental data from WIRINGA-1995 [36] and GRANADA-2016 [3].

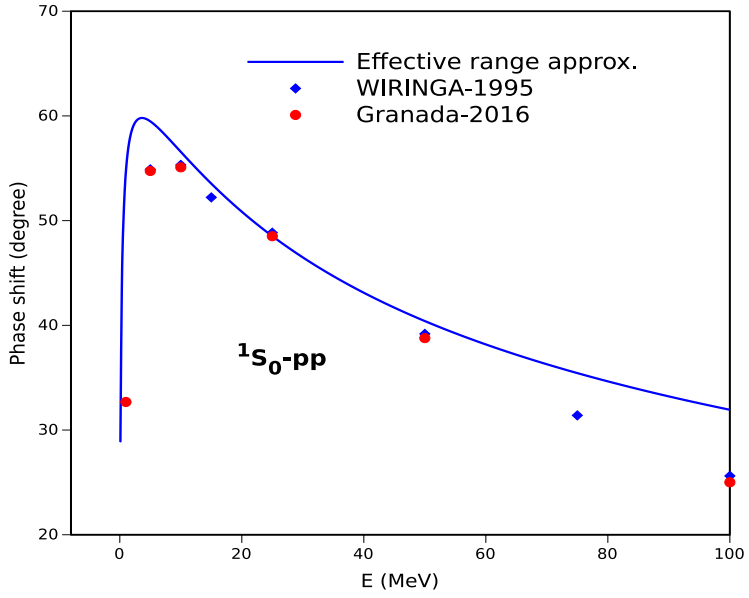

Fig. 6 – Singlet state ${}^1S_0 - pp$ phase shift variation in comparison to experimental data from WIRINGA-1995 [36] and GRANADA-2016 [3].

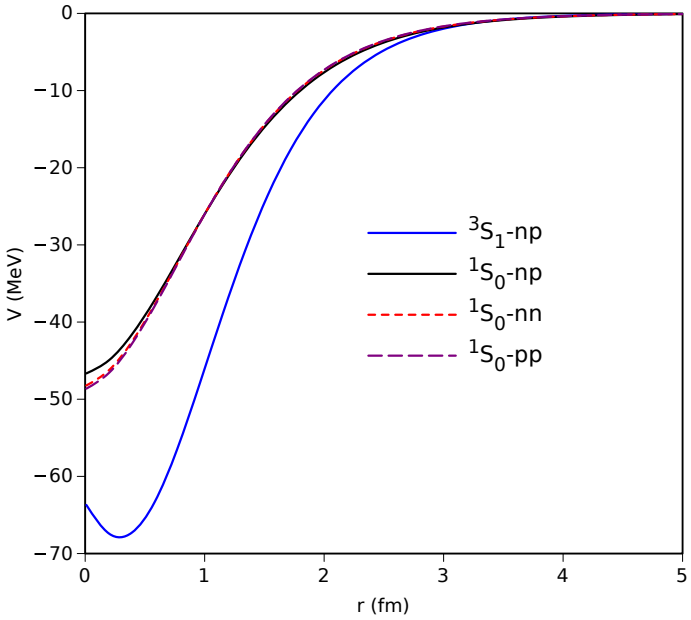

Fig. 7 – Potentials for $^3S_1$-np and $^1S_0$-np, nn & pp scattering systems.

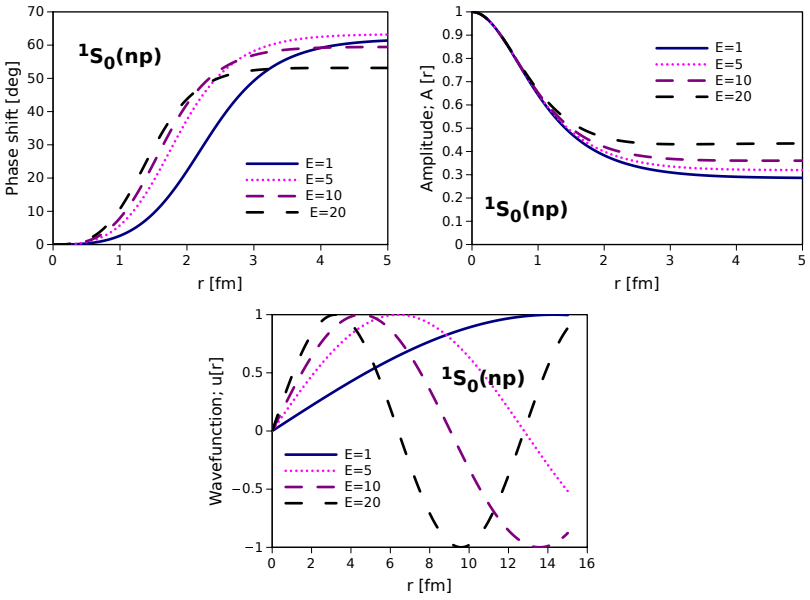

Fig. 8 – Phase shift $\delta(r)$, amplitude $A(r)$ and wave function u_0 *vs.* r for $^1S_0 - np$ system.

4. CONCLUSION

Using effective range approximation in variable phase approximation we obtained the scattering phase shifts for n-n, n-p and p-p scattering. Good match in SPS with experiment is found for energy upto 20 MeV after which deviations are seen for all $^1S_0$-(np, nn & pp) states. The reason for deviation in phase shift is that at very small inter-nucleon distances, a strong repulsive core is expected due to strong anti-correlation between nucleons hence the absence of the core is resulting into deviations observed in the scattering phase shifts. As stated by Breit *et al.*: "*Any of potential shapes like Square well, Gaussian well, exponential well and Yukawa well would give satisfactory agreement with the experimental data, provided the range and depth of the well are suitably chosen*". The presented potential is also exponential shaped and good enough to fit low energy SPS just by giving scattering parameters as inputs within variable phase approach.

Acknowledgements. This work is dedicated to Prof. Francesco Calogero for his wonderful book, "*Variable Phase Approach to Potential Scattering*."

REFERENCES

1. H. Yukawa, On the interaction of elementary particles, I, Proc. Phys. Math. Soc. Jpn. **17**, 48-57 (1935).
2. M. Naghdi, Nucleon-nucleon interaction: A typical/concise review, Phys. Part. Nucl. **45**, 924-971 (2014).
3. R. N. Perez, J. E. Amaro, and E. R. Arriola, The low-energy structure of the nucleon-nucleon interaction: statistical *versus* systematic uncertainties, J. Phys. G **43**(11), 114001 (2016).
4. S. Aoki, Hadron interactions in lattice QCD, Prog. Part. Nucl. Phys. **66**(4) 687-726 (2011).
5. H. Nemura, N. Ishii, S. Aoki, and T Hatsuda, Hyperon-nucleon potentials from lattice QCD, arXiv:0710.3622 (2007).
6. I. Slaus, Neutron-neutron interaction, Rev. Mod. Phys. **39**(3), 575 (1967).
7. M. Sarsour *et al.*, Measurement of the absolute differential cross section for np elastic scattering at 194 MeV, Phys. Rev. C **74**(4), 044003 (2006).
8. C. W. Akerlof, R. H. Hieber, A. D. Krisch, K. W. Edwards, L. G. Ratner, and K. Ruddick, Elastic proton-proton scattering at 90° and structure within the proton, Phys. Rev. **159**, 1138 (1967).
9. G. Darewych and A. E. S. Green, Morse function and velocity-dependent nucleon-nucleon potentials, Phys. Rev. **164**(4), 1324 (1967).
10. E. M. Henley and L. K. Morrison, n-n and n-p scattering lengths and charge independence, Phys. Rev. **141**(4), 1489 (1966).
11. V. A. Babenko and N. M. Petrov, Study of the low-energy characteristics of neutron-neutron scattering in the effective-range approximation, arXiv:1605.04849 (2016).
12. E. Konobeevski, Study of neutron-neutron scattering in nd breakup reaction, J. Phys. Conf. Ser. **340**(1), 012047 (2012).
13. A. P. Palov, and G. Gabriel Balint-Kurti, VPA: computer program for the computation of the phase shift in atom-atom potential scattering using the variable phase approach, Comput. Phys. Commun. **263** (2021).

14. G. Balassa, Estimating scattering potentials in inverse problems with Volterra series and neural networks, Eur. Phys. J. A. **58**(9), 186 (2022).
15. G. Balassa, Fixed-energy inverse scattering with radial basis function neural networks and its application to neutron–α interactions, Prog. Theor. Exp. Phys. **2023**(11),113A01 (2023).
16. A. Khachi and G. Balassa, Estimating Inverse Scattering Potentials for np System Using Variational Monte Carlo & Neural Networks, arXiv:2407.02137 (2024)
17. V.I. Zhaba, The variable phase approach: phase, amplitude and wave functions of the states for np-system for Argonne v18 potential, World Sci. News. **123** 161-180 (2019).
18. A. Khachi, Isospectral potentials and quantum mechanical functions for neutron-neutron scattering, arXiv:2309.16780 (2023).
19. A. Khachi, L. Kumar, M. R. Ganesh Kumar, and O. S. K. S. Sastri, Deuteron structure and form factors: Using an inverse potential approach, Phys. Rev. C **107**(6), 064002 (2023).
20. L. Kumar, S. Awasthi, A. Khachi, and O. S. K. S. Sastri, Phase shift analysis of light nucleon-nucleus elastic scattering using reference potential approach, arXiv:2209.00951 (2022).
21. S. Awasthi and O. S. K. S. Sastri, Real and imaginary phase shifts for nucleon-deuteron scattering using phase function method, arXiv:2304.10478 (2023).
22. A. Khachi, L. Kumar, and O. S. K. S. Sastri, Alpha-alpha scattering potentials for various channels using phase function method, Phys. At. Nucl. **85**(4), 382 (2022).
23. A. Khachi, S. Awasthi, L. Kumar, and O. S. K. S. Sastri, Algorithm to obtain inverse potentials for α-α scattering using variable phase approach, Comput. Math. Math. Phys. **64**(10), 2320 (2024).
24. A. Khachi, L. Kumar, A. Awasthi, and O. S. K. S. Sastri, Inverse potentials for all ℓ-channels of neutron-proton scattering using reference potential approach, Phys. Scr. **98**(9), 095301 (2023).
25. O. S. K. S. Sastri, A. Khachi, and L. Kumar, An innovative approach to construct inverse potentials using variational Monte-Carlo and phase function method: Application to np and pp scattering, Braz. J. Phys. **52**(2), 58 (2022).
26. A. Khachi, O. S. K. S. Sastri, L. Kumar, and A. Sharma, Phase shift analysis for alpha-alpha elastic scattering using phase function method for Gaussian local potential, J. Nucl. Phys. Mater. Sci. Radiat. Appl. **9**(1), 1-5 (2021).
27. A. Khachi and O. S. K. S. Sastri, ^{3}He-α elastic scattering phase shifts in various channels using phase function method with Morse potential, J. Nucl. Phys. Mater. Sci. Radiat. Appl. **9**(2), 161-167 (2022).
28. S. Awasthi, I. Kant, A. Khachi, and O. S. K. S. Sastri, Elastic scattering study of α-^{3}H and α-^{3}He modeled by Malfliet-Tjon potential using phase function method, Indian J. Phys. **99**, 347-355 (2024).
29. A. Sharma and O. S. K. S. Sastri, Numerical solution of Schrödinger equation for rotating Morse potential using matrix methods with Fourier sine basis and optimization using variational Monte-Carlo approach, Int. J. Quantum Chem. **121**(16), e26682 (2021).
30. A. Sharma, S. Gora, J. Bhagavathi, and O. S. K. S. Sastri, Simulation study of nuclear shell model using sine basis, Am. J. Phys. **88**(7), 576-85 (2020).
31. S. Gora, O. S. K. S. Sastri, and S. K. Soni, Optimization of semi-empirical mass formula coefficients using least square minimization and variational Monte-Carlo approaches, Eur. J. Phys. **43**(3), 035802 (2022).
32. A. Khachi, Phase shift, amplitude and wavefunctions for np-system using Morse potential by Calogero's approach, arXiv:2308.03824 (2023).
33. F. Calogero, Variable Phase Approach to Potential Scattering (Academic, New York, 1967).
34. V. V. E. Babikov, The phase-function method in quantum mechanics, Sov. Phys. Usp. **10**(3), 271 (1967).

35. P. M. Morse and W. P. Allis, The effect of exchange on the scattering of slow electrons from atoms, Phys. Rev. **44**(4), 269 (1933).
36. R. B. Wiringa, V. G. J. Stoks, and R. Schiavilla, Accurate nucleon-nucleon potential with charge-independence breaking, Phys. Rev. C **51**(1), 38 (1995).
37. A. Khachi, Computing scattering cross sections for spherically symmetric potentials, Am. J. Phys. **92**(7), 559-60 (2024).